Sensitivities in the acoustic modeling of damping materials for automobile applications

Maria Gavila Lloret[1], Ulrich Gabbert[2], Gregor Müller[1]

[1] *BMW Group, 80788 München, Deutschland, Email: Maria.Gavila-Lloret@bmw.de*

[2] *Otto-von-Guericke-Universität Magdeburg, 39106 Magdeburg, Deutschland*

Introduction

In the automotive industry the product design processes rely more and more on virtual methods as a consequence of shorter development cycles and the reduction of prototype hardware. Reliable statements at the early stages are only possible if the behavior of all the components is described in the models with sufficient accuracy. During the development of acoustic concepts, the modeling of the acoustic treatments is a decisive factor for a robust prediction of the sound transmission. These treatments are used to reduce the impact of the noise by absorption, insulation, damping or decoupling. Many of the passive noise control treatments present in automotive applications, as for example absorbers or spring-mass systems, include one or more layers of poroelastic materials. Poroelastic media are formed by an elastic solid frame whose pores are filled with a fluid. This biphasic nature gives the materials a complex, high dissipative behavior that makes them suitable as acoustic treatments. However, such behavior is also difficult to model, since the interactions between the two phases must also be considered, meaning an additional effort with respect to classical elastic and fluid media.

Numerous aspects must be considered when describing poroelastic media. A key factor for accurate results is the choice of the right material formulation. Furthermore, other influences like uncertainties in the input material properties or the coupling conditions to other components determine the robustness of the predictions. This article aims to analyze the extent to which these variable parameters affect the overall results. To that end, we study the response of a spring-mass system attached to a thin steel plate under airborne noise excitation, with a focus on the poroelastic middle layer. The next section reviews the common formulations to model poroelastic media and the required material properties, emphasizing on the sources of the parameters variability. After introducing the selected test setup, several influence factors are examined, including the material formulation, deviations in the input parameters and the impact of the coupling conditions. Here, experimental data serve as reference. Finally, the main findings are summarized.

Theoretical background

The theory of poroelasticity by Biot-Allard [1], [2] is the most extended approach to describe the sound propagation in elastic porous media. Its main underlying assumption is the homogenization. This means that, provided that the wavelengths of the waves propagating inside the material are much larger than the pores size, the biphasic aggregate can be treated as a homogeneous medium in which the two phases are simultaneously present. Consequently, the resolution of the pores on the microscale is avoided. The two governing equations have the form of a fluid-structure interaction problem with the particularity that the mechanical coupling between the elastic frame deformation and the fluid behavior is not limited to the fluid-structure interfaces, but is of a volume nature.

In the case that one of the two phases dominates the overall dynamics, it is possible to derive two simplifications directly from the coupled equations. On the one hand, if the elastic frame is just slightly excited, a fluid model may be sufficient. On the other hand, if the dissipation effects in the filling fluid are negligible, the material can be described as a classical elastic solid. The three formulations are in the following referred to as *poroelastic*, *porous* and *elastic*. The scope of application of each model is, however, not clearly limited and this is the main focus of the analyses in the next sections.

The parameters defining the equations coefficients can be grouped in three classes: fluid, elastic and poro-mechanical. The first set includes the material properties of the filling fluid, namely its density ρ_0, its viscosity η_0 and the speed of sound c_0. Elastic parameters characterize the response of the frame in vacuo, and are typically the Young's modulus E, the Poisson ratio ν, the structural damping coefficient η and the density of the drained material ρ_1. The poro-mechanical parameters help to link the microscopic thermal and viscous effects at a local level by changes in the macroscopic effective bulk modulus and the effective dynamic density. This requires a microscopic model as, for example, the one proposed by Johnson-Champoux-Allard (JCA [3], [4]), which is employed in our research. The input data needed for the JCA model are the open porosity ϕ, the airflow resistivity σ, the tortuosity α_∞, the viscous characteristic length Λ and the thermal characteristic length Λ'.

Some of the procedures to determine the values of these parameters can be found in [5], [6], [7] and [8]. We must point out that the characterization of poroelastic materials is associated with inaccuracies of different kind. First, the tested samples often include inhomogeneities as a result of the manufacture processes. Second, the measurement equipment and techniques employed suffer from reproducibility issues, as highlighted in [9]. Lastly, the use of elastic properties obtained from quasi-static tests is a common practice, but their value may differ significantly at higher frequencies [10]. The sensitivity of the material models to these variations is assessed here with help of some application examples.

Configuration setup

As aforementioned, the influence of the material models and the variability of the input parameters are investigated at the poroelastic middle layer of a spring-mass system attached to a thin steel plate. A diffuse pressure field excitation is directly applied to the steel plate. The vibroacoustic energy is transmitted and is, eventually, radiated in a semi-infinite receiving fluid. A sketch of the tested configuration is shown in Figure 1. This setup is of special interest because of its wide application as acoustic treatment in the automotive industry. Moreover, the location of the foam between the two structural components induces vibrations in the solid frame of the poroelastic material.

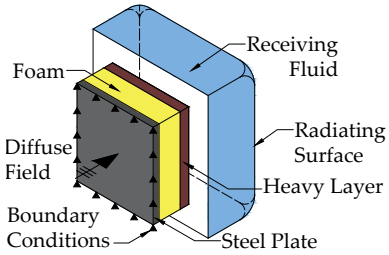

Figure 1: Schematic representation of the tested configuration. Note that the dimensions are not to scale.

The basis geometry is a one-meter square steel plate on which the spring-mass system is attached. For the finite element simulation with the commercial software Actran®, the steel plate and the mass layer (also called heavy layer) are discretized with solid shell elements, special elements for very thin plates that have three degrees of freedom (DOF) per node. A simply supported boundary condition is imposed by restraining the displacement of the nodes at the plate's edges in the thickness direction. The foam layer is discretized with hexahedral elements whose number of DOF depends on the formulation chosen for the poroelastic material: four DOF for the poroelastic (acoustic pressure and three displacement components), one for the porous (acoustic pressure) and three for the elastic model (three displacement components). The incident diffuse pressure field is directly applied on the outer surface of the steel plate. In order to model the free radiation condition, the heavy layer is coupled to a semi-infinite receiving fluid formed by a finite fluid volume modeled with infinite elements on its outermost layer. On this outer surface it is possible to retrieve the total power radiated by the system.

An equivalent spring-mass configuration has been measured in a window test bench for validation purposes. The test object, composed of a steel plate, a foam layer and a heavy layer, is located in the aperture connecting two rooms: a reverberation chamber in which a loudspeaker generates the diffuse field excitation, and a semi-anechoic room that ensures the free wave propagation on the receiving side. The radiated power of the system is calculated from the pressure and the velocity distributions measured with help of an array of PU-probes.

The response of two different spring-mass systems is examined below. Only the foam layer changes from one system to the other. The complete systems were first measured in the window test bench, and later the foam properties were determined by the methods referenced in the previous section. The results are the input data for the numerical models. The performance of each spring-mass system is evaluated in terms of its insertion loss (IL), which is defined as the difference between the radiated power W_{rad} of the bare steel plate and of the steel plate with a noise control treatment attached (NCT, see equation (1)). Regarding the system's frequency response, two important design criteria are used. They are the spring-mass resonance and the high frequency slope of the curve.

$$IL[dB] = W_{rad}^{bare}[dB] - W_{rad}^{NCT}[dB] \tag{1}$$

Besides the investigation of the suitability of the material models, the focus of the present research is to analyze to which extent the system's response is modified by variations in the input information. To quantify the sensitivity of the formulations to a given parameter we calculate the deviation from the reference values, analogous to the standard deviation (equation 2).

$$s = \sqrt{\frac{1}{N}\sum_{i=1}^{N}\left(IL_i^{var} - IL_i^{ref}\right)^2} \tag{2}$$

where N is the number of points in the frequency domain.

Results of the sound transmission through a spring-mass system

Next, we examine the performance of the different material models on two foams A and B. To that end, the description of the foam layer is selected from one of the three models introduced before. All other parameters, including the material properties, remain unchanged.

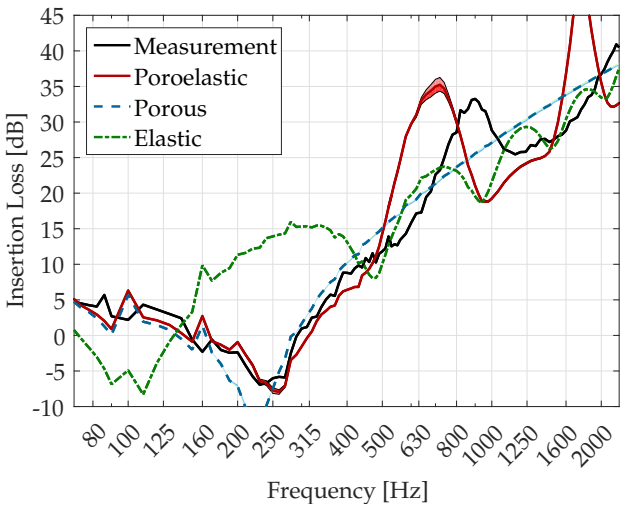

Figure 2: Comparison of the insertion loss results for the spring-mass system A, different material models for the foam. The colored areas correspond to a ±10% variation of the thermal characteristic length Λ'.

For the first foam material (we refer to the aggregate as *system A*) we can identify in Figure 2 that the poroelastic description gives the closest match to the measured data. The frequency and the level of the spring-mass resonance are correctly predicted and also the high frequency slope has an acceptable level. The too low predicted resonances and anti-resonances at higher frequencies may indicate the missing bulk stiffness in the numerical model for this frequency range. The porous simplification roughly follows the general trends, although it underestimates the damping at the spring-mass resonance and does not predict the high frequency resonances. That is because both effects are directly associated to the solid phase. The damping of the skeleton determines the resonance level, while the coincidence of entire shear wavelengths with the foam thickness are responsible for the high frequency resonances. Conversely, the elastic model gives a correct resonance level. Nevertheless, the value of the spring-mass resonance frequency is much lower than in the experimental data. The frequency at which the resonance appears is proportional to the material stiffness. Consequently, this shift indicates that the modeled elastic material is too soft. If compared to the apparent stiffness of the solid skeleton, the apparent stiffness of the air is one order of magnitude larger. Hence the simplification as an elastic solid for this foam lacks of the main contribution to the total stiffness. At higher frequencies the behavior of the elastic model is similar to the response observed for the poroelastic one, but with different resonance amplitudes. In summary, the poroelastic description is the best suited for this application, but the stiffness at higher frequencies should be modified to improve the match.

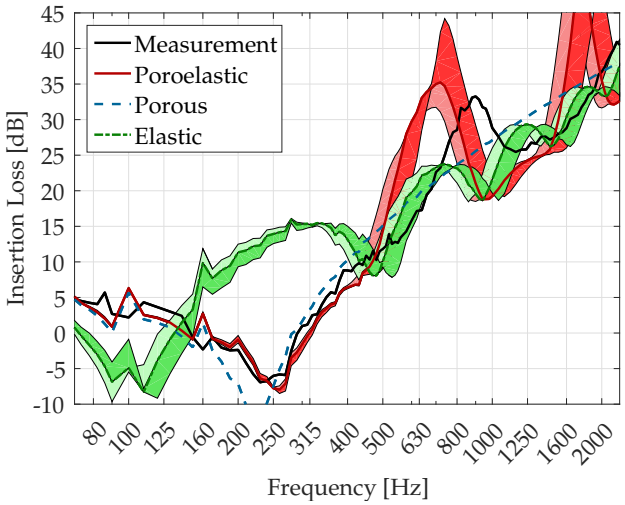

Figure 3: Comparison of the insertion loss results for the spring-mass system A, different material models for the foam. The colored areas correspond to a ±10% variation of the Poisson's coefficient ν.

For the foam characterization three specimens of the same material are employed. Later the results are averaged and the standard deviation are calculated. The differences in the measured parameters originate from inhomogeneities among the samples and from the instrument errors. For foam A we find the largest deviations in the Poisson's coefficient ν (11%), the thermal characteristic length Λ' (9%), and the Young's modulus E (7%). As a next step, we focus on the sensitivity of the models to these parameters by varying their value in a range around ±10% of the average. The results are displayed in Figure 3 for ν and in Figure 2 for Λ', in which the values between the minimum and maximum results have been colored. The darker colors correspond to the positive variation. One of the simplified models remains unchanged in each case, since the modified parameter is not present in that formulation. The trends when modifying the elasticity modulus are very similar to the behavior of a variation of the Poisson's ratio and, therefore not shown.

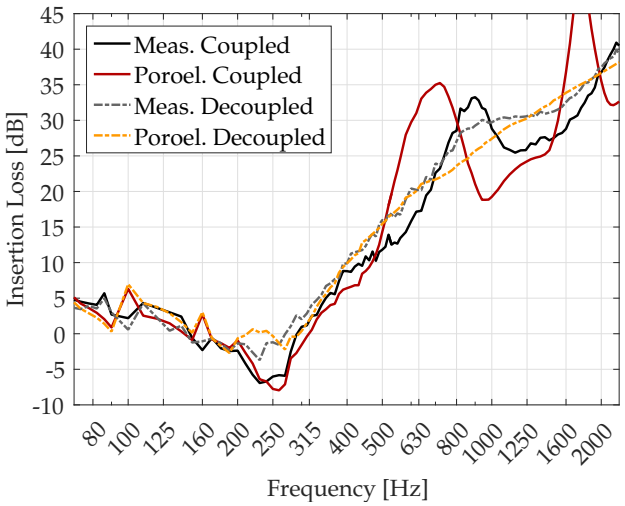

Figure 4: Comparison of the insertion loss results for the spring-mass system A with the poroelastic material model in the coupled and the decoupled state.

As displayed in Figure 3, an increase of the elastic parameter ν (or E) leads to a general curve shift towards higher frequencies and thus to a slightly better fit. In the case of the poroelastic modeling it is clearly seen that the location of the spring-mass resonance is for this material dominated by the stiffness of the fluid phase and, consequently, not influenced by the modification of the frame properties. The impact of the Poisson's ratio is larger, with a deviation s of 4.3 dB for the poroelastic model and 2.5 dB for the elastic formulation, whereas the sensitivity to the Young's modulus provides 3.2 dB and 1.7 dB, respectively. Oppositely, the variation of the thermal characteristic length Λ' has almost no visible effect on the overall results for none of the models (Figure 2), obtaining a s equal to 0.2 dB for both poroelastic and porous formulations. The sensitivity to other poromechanical parameters is low too and, hence, has been omitted here.

Another significant factor for a correct modeling is the adequate representation of the contact conditions. This effect is analyzed in Figure 4, where two coupling configurations are compared: the foam directly bonded to the steel plate (*Coupled*) and the separation by a thin air gap placed between the plate and the foam layer (*Decoupled*). The data displayed for the simulations are calculated with the poroelastic model, as it gives the best

correlation with the measured data for the two setups. In the decoupled state, the numerical model fails to reproduce the damped high frequency resonance, suggesting that the excitation of the solid phase is too low. In spite of that, the general correspondence between the experimental and numerical results is good and emphasizes the importance of the coupling conditions for accurate results. Further analyses have verified that the presence of the air gap reduces the excitation of the foam's frame. Consequently, its sensitivity to the elastic parameters diminishes. For example, a s value of only 0.4 dB results from a ±10% variation of the Young's modulus.

The second foam investigated (*system B*) has a higher Young's modulus than the first one, which implies differences in the system's behavior. As shown in Figure 5, the elastic formulation is the overall most appropriate model. It exhibits the closest correspondence to the measured IL curve, especially for the high frequency slope. However, the response at the spring-mass resonance is not accurately captured. Moreover, the curve drops above 1600 Hz. This of of the same nature as the high frequency resonances in the previous graphs, but it is not recognizable in the experiment. The poroelastic and porous models are better at the prediction of the frequency at which the spring-mass resonance occurs, but not at the IL resonance level. Furthermore, these two models overestimate the performance of the treatment significantly in the high frequency range.

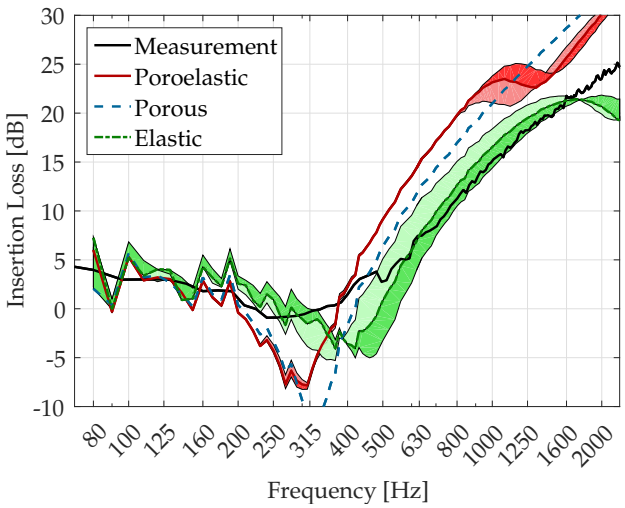

Figure 5: Comparison of the insertion loss results for the spring-mass system B, different material models for the foam. The colored areas correspond to a ±25% variation of the Young's modulus E.

Additionally, Figure 5 displays the system's response to a ±25% variation of the Young's modulus. This parameter has been selected because it provided a deviation during the foam's characterization measurements of 27%. The elastic model is more sensitive to this property (s = 2.3 dB by ±25% E), whereas the poroelastic formulation is only affected in the vicinity of the structural high frequency resonances and has a lower sensitivity (s = 1.2 dB). As a general rule, the modification of the material properties can help to improve the match of a model in a given frequency range, but does not considerably modify the curve shape of the system's frequency response.

Conclusions

The former examples illustrate the importance of the material model choice to achieve an accurate prediction of the sound transmission. The sensitivity of the models to the elastic parameters is found to be larger than to the poro-mechanical coefficients. The variation of the input parameters in the range of the deviations in the characterization measurements can enhance the correspondence with the experimental data in certain frequency ranges, especially at higher frequencies, provided that the proper material formulation is selected. Further analyses based on a wider selection of foam materials are required as next step to extend the application of these conclusions.

References

[1] Biot, M.A.: Theory of propagation of elastic waves in a fluid-saturated porous solid. I. Low frequency range, II. Higher frequency range, The Journal of the Acoustical Society of America 28 No 2 (1956) 168-191.

[2] Allard, J.F.: Propagation of sound in porous media. Modelling sound absorbing materials, Elsevier London, New York (1993).

[3] Johnson, D.L., *et al.*: Theory of dynamic permeability and tortuosity in fluid-saturated porous media, Journal of Fluid Mechanics 176 (1987) 379-402.

[4] Champoux, Y., Allard, J.F.: Dynamic tortuosity and bulk modulus in air-saturated porous media, Journal of Applied Physics 70 No 4 (1991) 1975-1979.

[5] Jaouen, L., *et al.*: Elastic and damping characterizations of acoustical porous materials: Available experimental methods and applications to a melamine foam, Applied Acoustics 69 No 12 (2008) 1129-1140.

[6] Salissou, Y., Panneton, R.: Pressure/mass method to measure open porosity of porous solids, Journal of Applied Physics 101 No 12 (2007) 124913.

[7] Atalla, Y., Panneton, R.: Inverse acoustical characterization of open cell porous media using impedance tube measurements, Canadian Acoustics 33 No 1 (2005) 11-24.

[8] ISO 9053:1991: Acoustics - Materials for acoustical applications - Determination of airflow resistance.

[9] Pompoli, F., *et al.*: How reproducible is the acoustical characterization of porous media?, The Journal of the Acoustical Society of America 141 No 2 (2017) 945-955.

[10] Van der Kelen, C., *et al.*: On the influence of frequency-dependent elastic properties in vibro-acoustic modelling of porous materials under structural excitation, Journal of Sound and Vibration 333 No 24 (2014) 6560-6571.